Inorganic Chemistry

ARTICLE

pubs.acs.org/IC

Semirigid Aromatic Sulfone−Carboxylate Molecule for Dynamic Coordination Networks: Multiple Substitutions of the Ancillary Ligands

Xiao-Ping Zhou,[†] Zhengtao Xu,[*,†] Matthias Zeller,[‡] Allen D. Hunter,[‡] Stephen Sin-Yin Chui,[§] and Chi-Ming Che[§]

[†]Department of Biology and Chemistry, City University of Hong Kong, 83 Tat Chee Avenue, Kowloon, Hong Kong, China

[‡]Department of Chemistry, Youngstown State University, One University Plaza, Youngstown, Ohio 44555, United States

[§]Department of Chemistry and HKU-CAS Joint Laboratory on New Materials, The University of Hong Kong, Pokfulam Road, Hong Kong, China

Supporting Information

ABSTRACT: We report dynamic, multiple single-crystal to single-crystal transformations of a coordination network system based on a semirigid molecule, TCPSB = 1,3,5-tri(4′-carboxyphenylsulphonyl)benzene, which nicely balances shape persistence and flexibility to bring about the framework dynamics in the solid state. The networks here generally consist of (1) the persistent core component (denoted as CoTCPSB) of linear Co^{II} aqua clusters (Co−O−Co−O-Co) integrated into 2D grids by 4,4′-bipyridine and TCPSB and (2) ancillary ligands (AL) on the two terminal Co^{II} ions—these include DMF (*N*,*N*′-dimethylformamide), DMA (*N*,*N*′-dimethylacetamide), CH_3CN, and water. Most notably, the ancillary ligand sites are highly variable and undergo multiple substitution sequences while maintaining the solid reactants/products as single-crystals amenable to X-ray structure determinations. For example, when immersed in CH_3CN, the AL of an as-made single crystal of CoTCPSB−DMF (i.e., DMF being the AL) is replaced to form CoTCPSB−CH_3CN, which, in air, readily loses CH_3CN to form CoTCPSB−H_2O; the CoTCPSB−H_2O single crystals, when placed in DMF, give back CoTCPSB−DMF in single-crystal form. Other selective, dynamic exchanges include the following: CoTCPSB−DMF reacts with CH_3CN (to form CoTCPSB−CH_3CN) but NOT with water, methanol, ethanol, DMA, or pyridine; CoTCPSB−H_2O specifically pick outs DMF from a mixture of DMF, DMA, and DEF; an amorphous, dehydrated solid from CoTCPSB−H_2O regains crystalline order simply by immersion in DMF (to form CoTCPSB−DMF). Further exploration with functional, semirigid ligands like TCPSB shall continue to uncover a wider array of advanced dynamic behaviors in solid state materials.

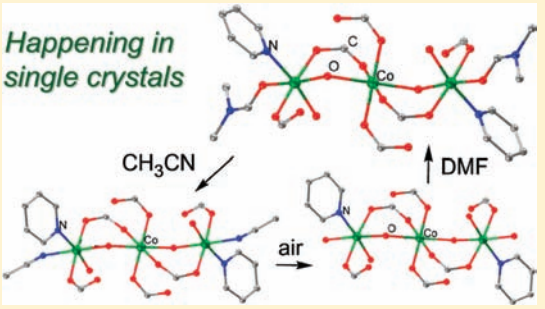

INTRODUCTION

Porous coordination networks (PCNs, or metal−organic frameworks, MOF),[1] constructed by using metal ions and organic linkers through coordination bonds, are attracting much attention for their remarkable porous features and potential application in sorption/separation,[2] catalysis,[2h,3] and sensing.[2e,4] Compared with the more rigid inorganic zeolites or metal oxides, the inherent suppleness of the organic building blocks tends to impart to the resultant coordination networks significant structural flexibility in the solid state, giving rise to dynamic behaviors in guest absorption and transport (e.g., guest molecules traversing a host net without open channels,[1f,5] sorption hysteresis), as well as in the conversions between different framework structures via external stimulus (e.g., heat, guest molecules)[5m,6] or solution/solvent-mediated processes.[7] On the other hand, the study of these dynamic behaviors can be greatly facilitated by the availability of crystallographical data, for example, single-crystal to single-crystal (SCSC) transformations can be monitored by X-ray crystal diffraction to unveil the relevant structural and mechanistic details.[5g]

Among the increasing number of reported SC−SC transformations of coordination networks,[5g,6a−6h,8] most are based on guest-dependent dynamic behaviors. To achieve reactions on the coordination spheres of the metal centers, heating is often needed to displace the volatile ancillary ligands (e.g., H_2O) by other donor species (e.g., carboxyl, pyridyl/MeOH, or NO_3^-).[6a−e] In these cases, the substituting donors often originate from the host network and they are usually preassembled around the metal center. By contrast, it remains a challenge to engage *externally* introduced guest ligands to effect substitution processes at the metal center, even though progress along this direction has recently been made by the groups of Bharadwaj[6h] and Zeng.[6g]

Received: April 8, 2011
Published: July 07, 2011

Scheme 1

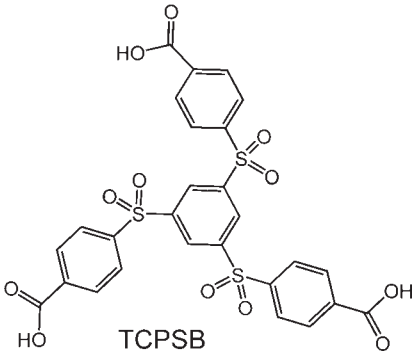

Scheme 2. Conversions among the Individual Phases of CoTCPSB[a]

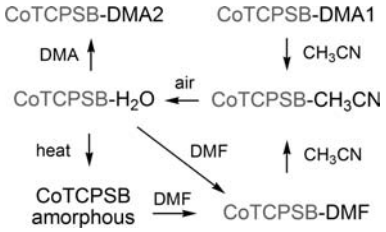

[a] CoTCPSB−DMA1 and CoTCPSB−DMF were first prepared solvothermally to initiate the conversion studies. We collected X-ray datasets for CoTCPSB−DMF (and CoTCPSB−CH_3CN) from two different batches of samples, e.g., labeled as CoTCPSB−DMF1 and CoTCPSB−DMF2. Except CoTCPSB−DMA1, which contains two types of 2D grids, all other single-crystal structures herein are isostructural and contain only one type of 2D grid.

The major novelty of this work lies in the development of molecular building block systems for tackling this challenge of exploring ancillary ligand substitution in coordination networks. As a general consideration, dynamic properties in solid state networks call for a balance between the degree of shape persistence and the conformational flexibility in the molecular building blocks, as the former generally imparts the strength and structural integrity of the host net while the latter allows for the concerted motion throughout the network to create the dynamic solid state properties. We thus conceived the molecule 1,3,5-tri(4′-carboxyphenylsulphonyl)benzene (TCPSB, Scheme 1) as a semirigid, tritopic building block equipped with two distinct sets of functions: (1) the commonly used carboxylate groups for building up the coordination scaffold and (2) the sulfone groups around the core of the molecule to bring about moderate flexibility and to play a functional role under certain circumstances (e.g., hydrogen-bond formation with the guest molecules or additional ligands).

The coordination networks reported here are based on a trinuclear Co(II) aggregate integrated by the linkers of TCPSB and 4,4′-bipyridine into 2D grids (denoted as CoTCPSB). Besides being bonded to the donor atoms from the linker molecules, the Co(II) centers can also bond to water and other small solvent molecules of DMA, DMF, and CH_3CN as ancillary ligands. The dynamic nature of the networks is mostly reflected in the multiple substitutions of the ancillary ligands (see Scheme 2 for an overview meant to help navigate the main text). Such substitution reactions proceed with both starting materials and products persisting in the form of single crystals, despite the lack of large open channel features in the single-crystal structures. Together with the significant changes in the lattice parameters, packing motifs of the layers, and local bonding features that accompanied the transformations, these observations point to the substantial cooperative motion of the atoms and molecules across the host lattice to accommodate the guest transport and the substitution processes.

EXPERIMENTAL DETAILS

Starting materials, reagents, and solvents were purchased from commercial sources (Aldrich and Acros) and used without further purification. Elemental analysis was performed by a Vario EL III CHN elemental analyzer. FT-IR spectra were measured using a Nicolet Avatar 360 FT-IR spectrophotometer. NMR spectra were measured using a Varian YH300 300 MHz superconducting-magnet NMR spectrometer using tetramethylsilane as the internal reference. Thermal analysis (TG) was carried out in a nitrogen stream using PerkinElmer STA6000 thermal analysis equipment with a heating rate of 10 °C min^{-1}. X-ray powder diffraction patterns of the bulk samples (the powder samples were spread onto glass slides for data collection) were collected at room temperature on a Siemens D500 powder diffractometer or Bruker D8 Advance diffractometer (Cu Kα, λ = 1.5418 Å).

Synthesis of 1,3,5-Tris(*p*-tolylthio)benzene (TTTB). In a nitrogen-filled glovebox, sodium 4-methylbenzenethiolate (3.285 g, 22.50 mmol) was loaded into a 100 mL two-neck round-bottom flask equipped with a septum. After the flask was taken out of the glovebox, DMEU (dimethylethyleneurea, 10.0 mL) was injected via cannula under nitrogen. When the sodium 4-methylbenzenethiolate was completely dissolved in DMEU, 1,3,5-trifluorobenzene (anhydrous, 0.660 g, 5.0 mmol) was added via cannula from a nitrogen-protected vial. The reaction mixture was then stirred and heated at 90 °C under nitrogen protection. After about 3 days, the orange-colored solution was poured into 100 mL of water and extracted with toluene (3 × 50 mL). The organic layers were then combined and washed with water (3 × 200 mL) and dried with anhydrous magnesium sulfate. The solvent was removed in vacuo, and the crude product was purified by flash chromatography (silica gel, hexanes) to provide a white solid (1.582 g, 71% based on 1,3,5-trifluorobenzene). ^{1}H NMR ($CDCl_3$, 300 MHz): δ 2.37 (s, 9 H), 6.75 (s, 3H), 7.08−7.11 (m, 6H), 7.24−7.27 (m, 6H). ^{13}C NMR ($CDCl_3$, 75 MHz): δ 21.48, 125.44, 129.43, 130.38, 133.64, 138.54, 140.04.

Synthesis of 1,3,5-Tris(tosyl)benzene. To a solution of 1,3,5-tris(*p*-tolylthio)benzene (0.250 g, 0.56 mmol) in dichloromethane (20.0 mL) was added *m*-chloroperbenzoic acid (85−95%, 0.614 g). The resultant solution was allowed to stir overnight at room temperature, after which it was diluted with dichloromethane (30.0 mL) and washed with a sodium hydroxide solution (10%, 2 × 50 mL), water (2 × 100 mL), and brine (100 mL). The organic layer was separated, dried with anhydrous magnesium sulfate, and concentrated in a vacuum to furnish 1,3,5-tris(tosyl)benzene (0.275 g, 91% based on 1,3,5-tris(*p*-tolylthio)benzene). ^{1}H NMR ($CDCl_3$, 300 MHz): δ 2.43 (s, 9 H), 7.33−7.35 (m, 6H), 7.78−7.81 (m, 6H), 8.51 (s, 3H). ^{13}C NMR ($CDCl_3$, 75 MHz): δ 17.95, 124.46, 126.28, 126.78, 132.63, 141.83, 142.05.

Synthesis of 1,3,5-Tri(4′-carboxyphenylsulphonyl)benzene (TCPSB). Dilute HNO_3 (5.80 g of 65% HNO_3 in 13.0 mL of water) was mixed with 1,3,5-tris(tosyl)benzene (100 mg, 0.185 mmol) and heated at 220 °C in a Teflon autoclave for 12 h. After cooling to room temperature and filtration, 87.5 mg of a white solid was obtained (75%, based on 1,3,5-tris(tosyl)benzene). ^{1}H NMR (300 MHz, DMSO-d_6): δ 8.08−8.11 (m, 6 H), 8.22−8.25 (m, 6 H), 8.71 (s, 3H). The solubility of TCPSB is very low in DMSO-d_6, and the ^{13}C NMR spectrum is not measured. IR (cm^{-1}): 3081w, 2986w, 2846w, 2666w, 2543w, 1698s, 1601w, 1576w,

dx.doi.org/10.1021/ic2007292 |*Inorg. Chem.* 2011, 50, 7142–7149

1489w, 1353m, 1343 m, 1286s, 1155s, 1123w, 1096w, 1079w, 1015w, 931w, 861w, 824 w, 806w, 763m, 713m, 687w, 665w, 621w, 601m, 583m, 567m, 555m, 446w.

Crystallization of CoTCPSB−DMF. A mixture of $Co(NO_3)_2 \cdot 6H_2O$ (3.0 mg), TCPSB (3.1 mg), 4,4′-bipyridine (3.6 mg), and DMF−water (1.0 mL, 4:1, v/v) was sealed in a glass tube, heated in an oven at 100 °C for 50 h, and slowly cooled to room temperature over a period of 12 h. Red block-like crystals were obtained (3.4 mg, 70%, based on TCPSB). Experiments on a larger scale (e.g., with 15.0 mg of TCPSB) in a large glass tube provided the same product (as checked by X-ray powder diffraction). Chemical analysis of the product $C_{77.5}H_{77.5}Co_3N_{6.5}O_{32.5}S_6$ (corresponding to $[Co_3(H_2O)_4(TCPSB)_2(bipy)(DMF)_2] \cdot 2.5DMF$) yields the following: Anal. Calcd C, 46.80; H, 3.93; N, 4.58. Found: C, 46.82; H, 3.64; N, 4.74.

Crystallization of CoTCPSB−DMA1. The procedure here is similar to that of CoTCPSB−DMF, except for the solvent (DMA−water, 4:1, v/v). Red block-like crystals were obtained (61%, based on TCPSB). Chemical analysis of the product (corresponding to $[Co_3(H_2O)_4(TCPSB)_2(bipy)(DMA)_2]_2 \cdot [Co_3(H_2O)_4(TCPSB)_2(bipy)] \cdot 8DMA \cdot 9H_2O$) yields the following: Anal. Calcd C, 46.58; H, 4.30; N, 4.07. Found: C, 46.29; H, 4.19; N, 4.33.

Preparations of CoTCPSB−CH_3CN. The crystals of CoTCPSB−DMF (10.0 mg) and CoTCPSB−DMA1 (10.0 mg) were immersed in acetonitrile (2.0 mL) for 2 days, and CoTCPSB−CH_3CN was obtained after filtration. After being exposed to air for 1 h, chemical analysis of the product found (C, 41.88; H, 3.67; N, 1.62), which closely matches CoTCPSB−H_2O ($C_{64}H_{66}Co_3N_2O_{38}S_6$, corresponding to $[Co_3(H_2O)_6(TCPSB)_2(bipy)] \cdot 8H_2O$) (calcd C, 41.77; H, 3.6; N, 1.52) and indicates that the CH_3CN in the solid sample has already been replaced by water.

Single-Crystal XRD Analyses. For CoTCPSB−DMF1, CoTCPSB−DMA1, CoTCPSB−CH_3CN2, and CoTCPSB−DMA2 data collections were conducted on a Bruker AXS SMART APEX CCD system using Mo Kα (λ = 0.71073 Å) radiation at 100(2) K. All absorption corrections were performed using the SADABS program. Crystals of CoTCPSB−CH_3CN1, CoTCPSB−H_2O, and CoTCPSB−DMF2 were studied on an Oxford Gemini S Ultra diffractometer. The crystals of CoTCPSB−CH_3CN1 and CoTCPSB−CH_3CN2 were immediately placed into grease after removal from the mother liquors. The crystals of CoTCPSB−H_2O are obtained by exposing CoTCPSB−CH_3CN crystals to air for about 1 h. The structures of CoTCPSB−DMF1 and CoTCPSB−DMA1 were solved by direct methods using SHELXTL 6.14 (Bruker AXS Inc., Madison, WI, 2003). All other structures were solved by isomorphous replacement starting with the structure of CoTCPSB−DMF1 under omission of the auxiliary ligands. All structures were refined by full-matrix least-squares on F_o^2 using SHELXTL 6.14. For summaries of the X-ray crystallographic data, see Tables S1−S4, Supporting Information. CCDC 812036−812042 (in the same order as listed in Tables S1−S4, Supporting Information) contain the supplementary crystallographic data for this paper. These data can be obtained free of charge from The Cambridge Crystallographic Data Centre via www.ccdc.cam.ac.uk/datarequest/cif.

RESULTS AND DISCUSSION

The first compound, CoTCPSB−DMF, with a network composition of $Co_3(H_2O)_4(TCPSB)_2(bipy)(DMF)_2$ was obtained in a solvothermal synthesis from $Co(NO_3)_2 \cdot 6H_2O$, 4,4′-bipyridine, and TCPSB with a mixture of DMF (*N*,*N*′-dimethylformamide) and water as the solvent. This compound crystallizes in the space group *P*−1 and features centrosymmetric, linear trinuclear Co^{II} aqua clusters (Co1−O−Co2−O−Co1) integrated into a 2D open network by the linkers TCPSB and 4,4′-bipy, as shown in Figure 1. The asymmetric portion of the unit cell of CoTCPSB−DMF contains 1.5 Co^{2+}

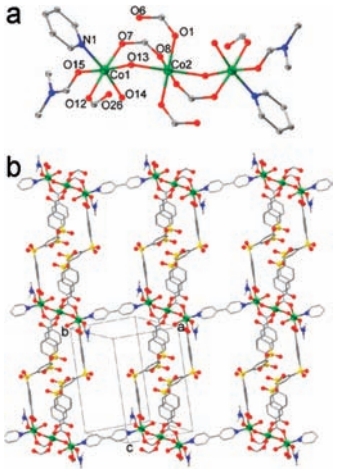

Figure 1. Co^{2+} coordination environments in CoTCPSB−DMF (a) and the resultant 2D grid (b).

centers and one TCPSB ligand, one-half of a 4,4′-bipy ligand, two H_2O units (one bridging Co1 and Co2, and the other bonded to Co1), and two DMF molecules (one bonded to Co1 and the other being noncoordinated). Both Co^{2+} atoms adopt an octahedral geometry. Co1 is bound by 5 oxygen atoms (i.e., O7 and O12 from TCPSB, O13 and O14 from water, and O15 from DMF; Co−O distances 2.022−2.214 Å; see Figure 1a) and one N atom of 4,4′-bipy (Co−N1, 2.116 Å); Co2 is bound by six oxygen atoms (e.g., O1 and O8 from TCPSB and O13 from water; Co−O distances 1.920−2.227 Å, Figure 1a). The bridging/bonding patterns of the carboxylate and aqua groups on the trinuclear Co(II) cluster are similar to that of a reported trinuclear Co^{2+} cluster.[9] Topologically, the Co(II) cluster can be considered a 4-connected node integrated by two types of linear struts into a 2D parallelogram net. One type of strut is provided by a single bipy molecule, while the other by a pair of TCPSB molecules is aligned in a parallel, centrosymmetric fashion. Such a complex linear link is partly made possible by the flexible conformation of the individual TCPSB molecules, which allows two of its branches to converge onto one metal cluster (the other branch being bound to another cluster). The 2D coordination grid contains significant cavities (Figure 1b) in which the noncoordinated DMF guests are located. On switching the solvent from DMF to DMA, one obtains, under similar conditions, CoTCPSB−DMA1, which, like CoTCPSB−DMF, also crystallizes in the space group *P*−1 and features linear trinuclear cobalt clusters integrated into 2D open networks by the TCPSB and bipy linkers (Figure 2). However, CoTCPSB−DMA1 manifestly differs from CoTCPSB−DMF (and other structures reported herein) in that it consists of not one but two types of 2D coordination grids, each with different coordination environments around the trinuclear cobalt clusters, as shown in Figure 2c and2d. The network composition for type I is $Co_3(H_2O)_4(TCPSB)_2(bipy)(DMA)_2$ and for type II $Co_3(H_2O)_4(TCPSB)_2(bipy)$. The trinuclear cobalt cluster in type I is similar to the cluster in CoTCPSB−DMF, except that DMA now takes the place of the DMF molecules (Figure 2a). Type II, by comparison, is not associated with any DMA ligands, with a carboxylate oxygen atom from one of the TCPSB molecules filling in to maintain the octahedral geometry. As a result, the adjacent Co atoms here (i.e., Co4 and Co5 of Figure 2b) are bridged by two carboxylate groups (c.f., one single bridging carboxylate in type I), with a

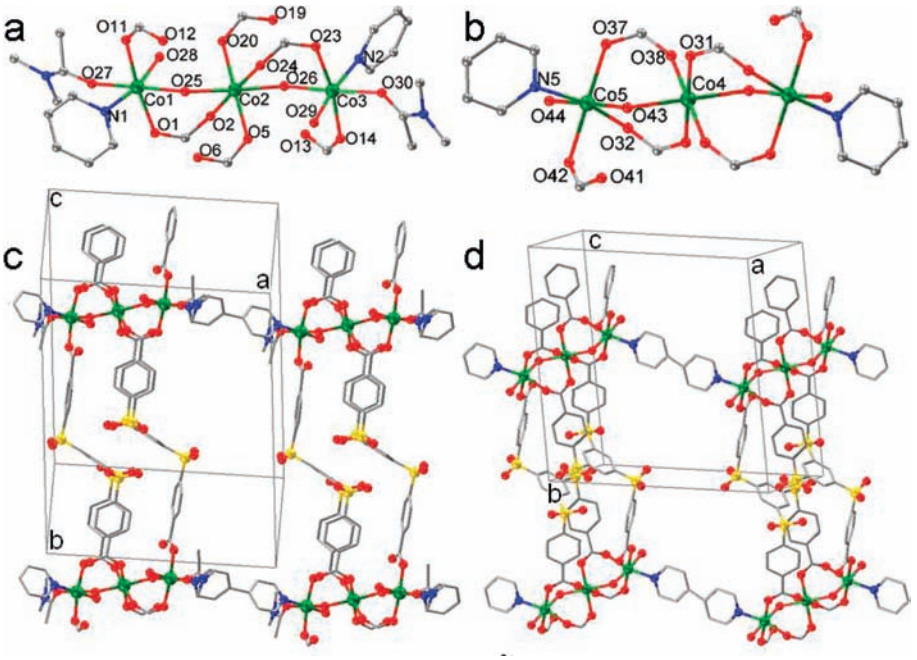

Figure 2. Coordination environments of the Co^{2+} ions in CoTCPSB−DMA1 (a, b) and the corresponding 2D grids ((a and c) type I and (b and d) type II).

shorter Co−Co distance of 3.585 Å (c.f., 3.700 and 3.706 Å in type I; see also Figure 2b). Networks of type I (the ones with DMA ligands) and type II (without DMA) do not occur in equal numbers—the ratio is 2:1. In other words, type I nets aggregate in pairs that alternate with the single nets of type II along the stacking direction (the *c* axis). In the cavities of the crystal structure are found the guests of DMA and water molecules.

When immersed in acetonitrile, single crystals of both CoTCPSB−DMF and CoTCPSB−DMA1 transformed into the new compound of CoTCPSB−CH_3CN in the single-crystal form: the crystal derived from CoTCPSB−DMF is labeled as CoTCPSB−CH_3CN1 and the crystals from CoTCPSB−DMA1 CoTCPSB−CH_3CN2. X-ray diffraction studies on both batches of CoTCPSB−CH_3CN crystals revealed that they are of the same structure, containing one single type of coordination grid that is isostructural to the above CoTCPSB−DMF but with the DMF molecules replaced by CH_3CN (Figure 3a and 3c) to give a network composition of $Co_3(H_2O)_4(TCPSB)_2(bipy)\text{-}(CH_3CN)_2$. In fact, CoTCPSB−$CH_3CN$ (and the other structures in the rest of the paper) was refined with the framework of the DMF-containing precursor as the starting point. Taken together, the three types of precursor networks—the one in CoTCPSB−DMF, type I and type II in CoTCPSB−DMA1—can all transform into this new net in CoTCPSB−CH_3CN. Notably, the transformation of the type II network in CoTCPSB−DMA1, which does not contain coordinated DMA molecules, involves more drastic motions in bond breaking/formation (e.g., displacing one carboxylate O atom by CH_3CN on Co5 and rearranging its coordination sphere) as well as in the conformational change of the TCPSB molecules.

It should be noted here that attempts to directly synthesize CoTCPSB−CH_3CN from $Co(NO_3)_2\cdot 6H_2O$ and TCPSB (using CH_3CN as the solvent) were not successful, suggesting that a dissolution/recrystallization process was unlikely to be involved in going from CoTCPSB−DMF (or CoTCPSB−DMA1) to CoTCPSB−CH_3CN, and thus, lending further evidence to support a single-crystal to single-crystal nature of the above transformations. Also, the formation/crystallization of the main framework from solution seems to be highly dependent on the templating molecules, with CH_3CN not being a suitable template in contrast to DMF or DMA. The transition from the liquid/solution state to the solid state network often involves exceptionally complicated processes, and a mechanistic account for the different templating effects of CH_3CN vs DMF and DMA is beyond this work. However, from the crystal structures one can infer to some degree the potential roles played by the steric and other local interactions on the ancillary ligand substitution processes. For example, the coordinated water molecules adjacent to DMF in CoTCPSB−DMF (O14) or DMA in CoTCPSB−DMA1 (O28, O29) on Co^{2+} centers were very stable; they were not substituted by acetonitrile. This stability appears to be consistent with the steric situation (the area around this aqua ligand is crowded by the neighboring groups, whereas the site of the CH_3CN ligand is less obstructed, see also Figures 1a and 2a) and the strong hydrogen bonding between the water and carboxylate group (e.g., the shortest hydrogen-bond distances for the water O14−O1 in CoTCPSB−DMF and O28−O20, O29−O5 in CoTCPSB−DMA1 are all under 2.74 Å).

When we performed IR measurements of the newly formed CoTCPSB−CH_3CN crystals (ground in air), we were surprised by the absence of the C≡N stretching peak (from CH_3CN) in the spectrum (Figure S1, Supporting Information), even though the disappearance of the characteristic peak of the C═O stretching of DMF at 1652 cm^{-1} (the peak of C═O vibration of DMA is overlapped with the peak of the network) and the methyl C−H stretching at 2930 cm^{-1} is within expectations. Also, the X-ray powder pattern of the CoTCPSB−CH_3CN crystals that were ground in air differs substantially from the one simulated from the single-crystal structure of CoTCPSB−CH_3CN (Figure 4). These observations suggest that the CoTCPSB−CH_3CN crystals very probably have transformed into a new phase after being exposed to air. Fortunately, the new

dx.doi.org/10.1021/ic2007292 |*Inorg. Chem.* 2011, 50, 7142–7149

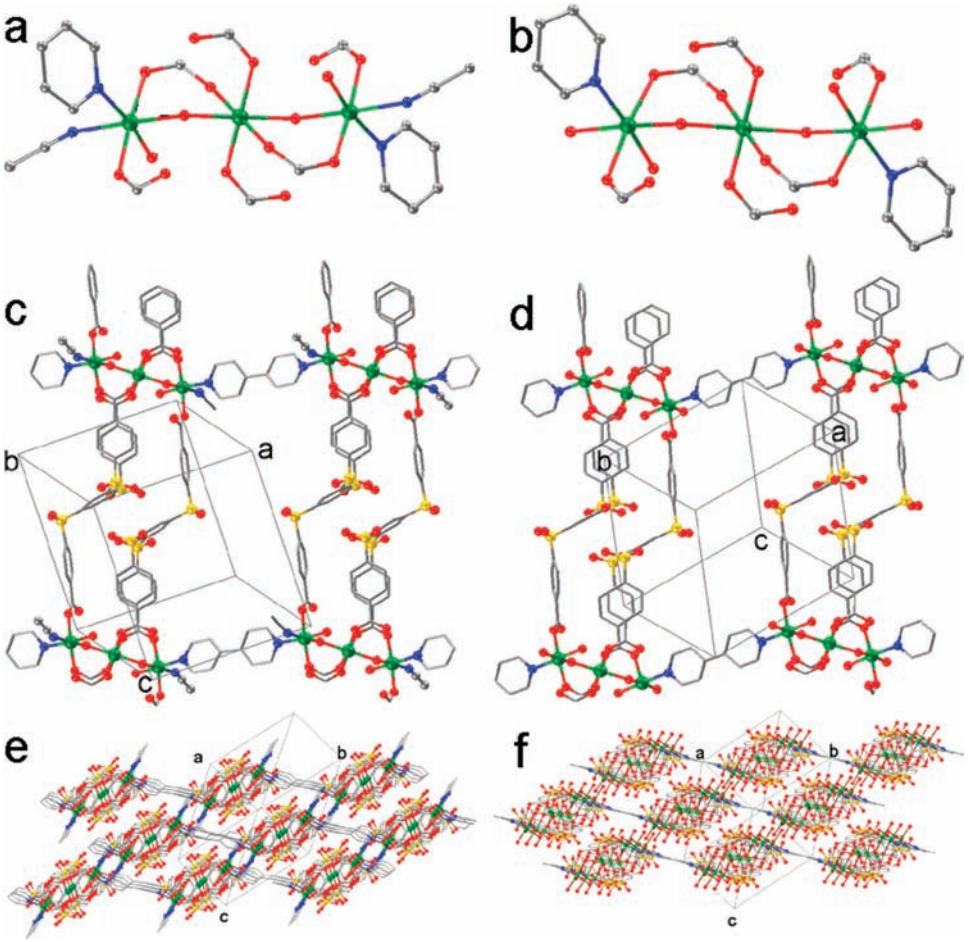

Figure 3. Coordination environment of Co^{2+} (a) and grid network in CoTCPSB−CH_3CN (c); coordination environment of Co^{2+} (b) and grid-like network in CoTCPSB−H_2O (d); packing of the 2D coordination nets in CoTCPSB−CH_3CN (e) and CoTCPSB−H_2O (f). Color code for atoms: green, Co; red, O; blue, N; gray, C; yellow, S.

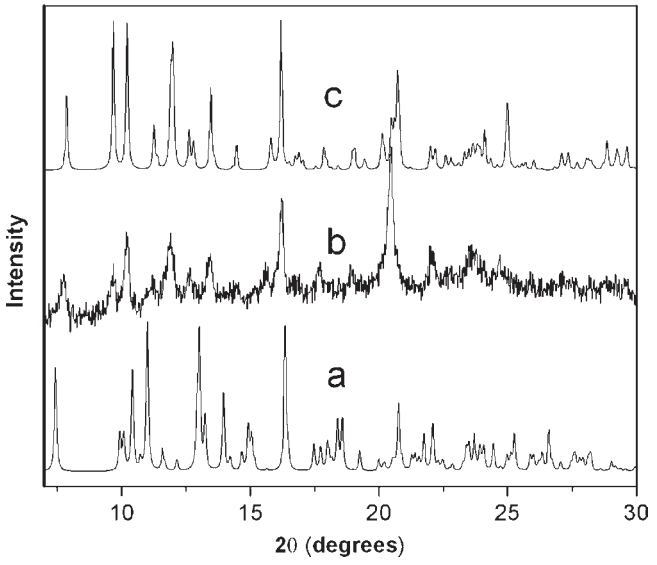

Figure 4. X-ray powder patterns (Cu Kα, λ = 1.5418 Å) (a) of the calculated pattern from the single-crystal structure of CoTCPSB−CH_3CN (data collected at 100 K), (b) observed from an as-made sample of 'CoTCPSB−CH_3CN' at 298 K, (c) of calculated pattern from the single-crystal structure of CoTCPSB−H_2O (data collected at 173 K).

phase can be determined by single-crystal X-ray diffraction (i.e., the single crystallinity of the mother CoTCPSB−CH_3CN crystals was preserved in this transformation), which reveals that the CH_3CN ligands in CoTCPSB−CH_3CN have been substituted by water molecules to form the new compound CoTCPSB−H_2O (Figure 3b and 3d), with a network composition of $Co_3(H_2O)_6(TCPSB)_2(bipy)$. The single-crystal structure of CoTCPSB−H_2O thus accounts for the absence of the CH_3CN peak in the IR spectrum, and the simulated X-ray powder pattern matches nicely with the observed pattern as shown in Figure 4. Furthermore, elemental analysis data also closely matched the CH_3CN-free structure from X-ray diffraction data, thus further indicating the expulsion of the CH_3CN molecules from the crystals of CoTCPSB−CH_3CN after being exposed to air.

The coordination network of CoTCPSB−H_2O is topologically similar to that of CoTCPSB−CH_3CN, with water molecules taking the place of CH_3CN as an ancillary ligand. Compared with the three progenitor systems, the "parallelogram window" of the 2D network in CoTCPSB−H_2O (Figure 5) is significantly "squashed". Specifically, while the parallelogram in CoTCPSB−H_2O features an acute angle of 66.31°, the figure in the other phases rises by about 10° to a range between 74° and 78°. Also, the 2D coordination networks of CoTCPSB−H_2O appear to be stacked in a more compact fashion, with significant

dx.doi.org/10.1021/ic2007292 |*Inorg. Chem.* 2011, 50, 7142–7149

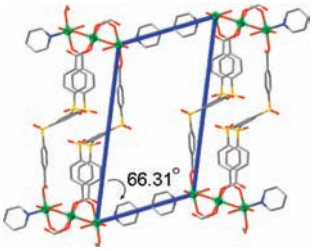

Figure 5. Parallelogram window in the network of CoTCPSB−H_2O (color code for atoms: green, Co; red, O; blue, N; gray, C; yellow, S).

hydrogen bonds between the sulfone groups and the aqua ligands across the 2D sheets (O−O distance = 2.961 Å, see also Figure 3f). Notice that the interlayer hydrogen bond entails the newly introduced aqua ligand (i.e., the one taking the place of the CH_3CN ligand) and might contribute, in part, to the facile transformation from CoTCPSB−CH_3CN to CoTCPSB−H_2O by means of "locking in" the aqua ligand. This is contrary to a recently reported 3D porous manganese coordination network in which departure of the CH_3CN ligands entailed heating at about 210 °C.[6h]

In contrast to the sensitivity of CoTCPSB−CH_3CN, the mother crystals of CoTCPSB−DMF and CoTCPSB−DMA1 (reminder: they both convert to CoTCPSB−CH_3CN in CH_3CN) are stable in air, and TGA studies (Figure S2, Supporting Information) showed that they start to lose the DMF or DMA molecules at about 117 and 133 °C, respectively. After immersing the crystals of CoTCPSB−DMF and CoTCPSB−DMA1 in water for 2 days, both IR and X-ray powder diffraction measurements indicated that the crystalline phase of CoTCPSB−DMF remains unchanged (Figure S3, Supporting Information), while the crystals of CoTCPSB−DMA1 become amorphous (Figure S4, Supporting Information). These tests indicate that direct transformation from CoTCPSB−DMF or CoTCPSB−DMA1 to CoTCPSB−H_2O is not as straightforward as from CoTCPSB−CH_3CN, and acetonitrile is a useful medium for preparing the phase of CoTCPSB−H_2O.

We also tested the potential exchange reactions of CoTCPSB−DMF toward other solvent molecules (e.g., methanol, ethanol, DMA, and pyridine) in procedures similar to the treatment with acetonitrile and water. The crystals of CoTCPSB−DMF remain visually unchanged in these tests, and the IR spectra do not exhibit significant new features, with the characteristic peaks (e.g., 1652 cm^{-1}) of DMF persisting in the spectra (Figure S5, Supporting Information). These tests indicate a particularly strong binding of the DMF to the Co(II) center, which can be ascribed to (1) the donor ability of its amide O atom (due to abetment from the N lone pair; by comparison, H_2O, methanol, and ethanol are weaker donors) and (2) its smaller size (e.g., relative to DMA) that reduces steric hindrance with the neighboring groups.

On the other hand, these tests also serve to highlight acetonitrile in its particularly strong ability to dislodge DMF from the host net. We suspect that such ability is associated with the linear, slender shape of CH_3CN and its open, unobstructed nitrile lone pair (also a better donor than the O atoms in water and alcohols), which serves to minimize the steric hindrance in the substitution process. By comparison, the lone pair on pyridine is flanked by two carbon groups, and it is therefore not as approachable. Notice that such steric agility is like a double-edged sword in that it could also facilitate the departure of the CH_3CN, as illustrated in its rapid replacement by H_2O in open air (to form CoTCPSB−H_2O). Replacement of CH_3CN by H_2O is, evidently, also facilitated by its volatility as well as the plenitude of H_2O in open air, which serves to push forward the transformation into CoTCPSB−H_2O.

Can CoTCPSB−H_2O be reverted to CoTCPBS−DMF or CoTCPBS−DMA1? For this, crystals of CoTCPSB−H_2O were immersed in DMF or DMA at room temperature for 1 day (for DMF) and 3 days (for DMA), respectively, and the resultant crystals (labeled as CoTCPBS−DMF2 and CoTCPBS−DMA2, respectively) were subjected to single-crystal X-ray diffraction studies. It turns out that CoTCPBS−DMF2 is of the same structure as the originally characterized CoTCPBS−DMF, with the aqua ligand (Figure 3b, O15, cis to the pyridine ring) in CoTCPSB−H_2O changed back to DMF. The reversion of CoTCPSB−H_2O to CoTCPSB−DMF was also supported by the IR spectra, which exhibit almost identical features between CoTCPBS−DMF2 and the originally prepared CoTCPBS−DMF (Figure S6, Supporting Information). In short, one achieves a full cycle from CoTCPSB−DMF to CoTCPSB−CH_3CN, then to CoTCPSB−H_2O, and finally back to CoTCPSB−DMF (Scheme 2).

The product of CoTCPBS−DMA2 features a structure similar to CoTCPSB−DMF (with DMA taking the place of DMF) but is structurally different from the originally prepared CoTCPBS−DMA1 (recall that CoTCPBS−DMA1 contains two types of networks, type I with DMA ligands and type II without). In other words, CoTCPBS−DMA2 only contains the type I network of CoTCPBS−DMA1. Thus, DMA is able to replace the water molecules in CoTCPSB−H_2O to generate CoTCPBS−DMA2 but unable to recover the original structure of CoTCPBS−DMA1 (Figure S7, Supporting Information). The difficulty in converting CoTCPSB−H_2O back to CoTCPBS−DMA1 is likely due to the more complex structure of the latter, which consists of two different types of networks stacked in a highly ordered manner (i.e., pairs of type I alternating with single nets of type II). To revert the simpler structure of CoTCPSB−H_2O to CoTCPBS−DMA1 would require the DMA molecules to differentiate, in a correspondingly highly ordered manner, the homologous layers of CoTCPSB−H_2O. Such an increase in orderliness seems very unlikely to occur simply by immersion at room temperature.

Out of curiosity, we then immersed the crystals of CoTCPSB−H_2O in a mixture of equal volumes of DMF, DMA, and DEF (*N*,*N*-diethylformamide). After 3 days, the IR spectrum features the peak of the characteristic C═O stretching of DMF at 1654 cm^{-1} (Figure S8a, Supporting Information) and solution ^1H NMR measurement (by dissolving the resultant crystals in a DCl/D_2O/DMSO-d_6 mixture) indicates that only DMF molecules from the ternary mixture were taken up by the host net (Figure S8b, Supporting Information). Thus, a strong selectivity in favor of DMF (relative to DMA and DEF) was observed of CoTCPSB−H_2O, which could be due to its smallest size among the three homologues. Further experiments also found that unlike DMF and DMA the largest size DEF does not replace the water molecules of CoTCPSB−H_2O under similar conditions (see the IR spectra in Figure S9, Supporting Information, and the PXRD patterns in Figure S10, Supporting Information). Preferential uptake of small-sized molecules observed of CoTCPSB−H_2O is quite common among porous coordination networks.[2e,6h,10] For example, a reported 3D porous manganese coordination network

dx.doi.org/10.1021/ic2007292 |*Inorg. Chem.* 2011, 50, 7142–7149

selectively takes up acetonitrile and not the larger molecules of acrylonitrile and allylnitrile.[6h]

Thermogravimetric analysis (TGA, Figure S11, Supporting Information) of the as-made sample of CoTCPSB−H_2O reveals a 11.8% weight loss at 146 °C, which corresponds to evacuation of 8 guest and 4 coordinated water molecules per formula unit of $[Co_3(H_2O)_6(TCPSB)_2]\cdot[bipy]]\cdot 8H_2O$ (calculated guest and coordinated water molecules (bridge water is not included) proportion in CoTCPSB−H_2O 11.7%), and no significant further weight loss was observed up to 381 °C. In fact, heating the crystals of CoTCPSB−H_2O under N_2 atmosphere at 100 °C for 2 h led to a color change from pink to purple, and the purple changes back to pink after exposure to air overnight (see Figure 6); this color change can be repeated multiple times and is reminiscent of $CoCl_2\cdot 6H_2O$, which changes from pink to deep blue upon dehydration. In addition, similar color changes associated with dynamic guest exchanges have been earlier observed in a Co(II)-based coordination polymer system.[11]

Powder X-ray diffraction study reveals that both the sample heated at 100 °C and the subsequent pink sample recovered from exposure in air lost crystallinity (see Figure 7b, for example). In spite of the loss of crystallinity, the reversible color changes (i.e., pink to purple, and purple to pink) persist in the amorphous sample (as shown by repeating the heating/air exposure cycle three times). More interestingly, like the crystalline mother compound CoTCPSB−H_2O, these noncrystalline powder samples change to the crystalline phase of CoTCPSB−DMF after being immersed in DMF at room temperature for 3 days (Figure 7c). Such a transformation suggests that the amorphous structure probably retains certain structural information from the crystalline mother compound of CoTCPSB−H_2O: information that serves to program the reestablishment of an isostructural crystalline network upon immersion in DMF. We should caution that it is generally difficult to completely rule out a dissolution/recrystallization mechanism in a transformation as above, even though in this particular case we can draw some assurance from the fact that the crystals of CoTCPSB−DMF were obtained under hydrothermal conditions and the direct mixing of the starting materials at room temperature does not result in the crystalline phase of CoTCPSB−DMF. The regaining of crystalline order from an amorphous solid sample has also been reported in several other systems[5d,10a,11,12] and in general reflects the structural flexibility of the networks.

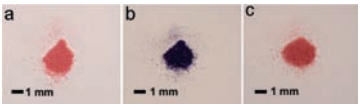

Figure 6. Photograph of the crystals of CoTCPSB−H_2O (a), the solids after heating at 100 °C for 2 h (b), and the solids after being exposed in air overnight (c).

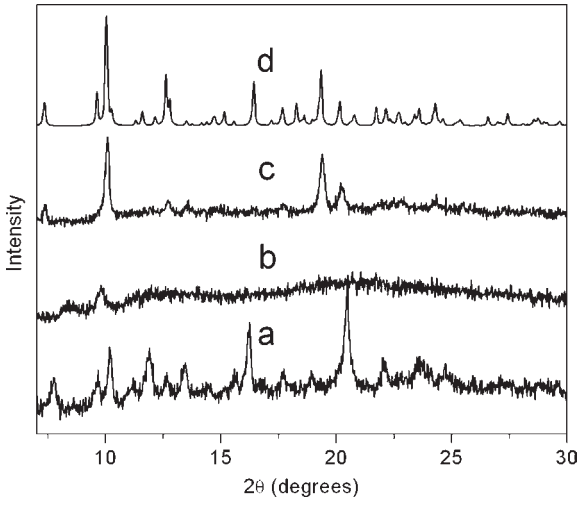

Figure 7. X-ray powder patterns (Cu Kα, λ = 1.5418 Å) (a) observed of an as-made sample of CoTCPSB−H_2O at 298 K, (b) observed of a solid sample of CoTCPSB−H_2O after heating at 100 °C for 2 h at 298 K, (c) observed of a sample of b immersed in DMF for 3 days at 298 K, and (d) a calculated pattern from the single-crystal structure of CoTCPSB−DMF (dataset collected at 100 K).

CONCLUSION

Multiple ligand substitution reactions at the cobalt centers can be carried out in the dynamic coordination network of CoTCPSB. Such reactions take place with both the reactant and the product networks in the form of single crystals and serve to highlight the remarkable structural flexibility that is imparted to the host network by the molecule TCPSB as a semirigid building block. Other interesting properties of the versatile host net of CoTCPSB uncovered in this exercise include the following: CoTCPSB−DMF selectively absorbs and reacts with acetonitrile in preference to water, methanol, ethanol, DMA, and pyridine; CoTCPSB−H_2O specifically pick outs DMF from a mixture of DMF, DMA, and DEF; the amorphous, dehydrated solid from CoTCPSB−H_2O regains crystalline order (and forms CoTCPSB−DMF) simply by immersion in DMF. Further exploration with functional, semirigid ligands like TCPSB shall continue to uncover a wider array of advanced dynamic behaviors in the resultant solid state framework materials.

ASSOCIATED CONTENT

Supporting Information. Full crystallographic data in CIF format, additional powder X-ray diffraction patterns, TGA plots, IR spectra, and solution NMR data. This material is available free of charge via the Internet at http://pubs.acs.org.

AUTHOR INFORMATION

Corresponding Author
*E-mail: zhengtao@cityu.edu.hk.

ACKNOWLEDGMENT

This work was supported by City University of Hong Kong (Project No. 7002471) and the Research Grants Council of HKSAR [Project 9041212 (CityU 103407)]. The single-crystal diffractometer at YSU was funded by NSF grant 0087210, the Ohio Board of Regents grant CAP-491, and Youngstown State University.

REFERENCES

(1) Selected reviews: (a) Chen, B.; Xiang, S.; Qian, G. *Acc. Chem. Res.* **2010**, *43*, 1115. (b) Thomas, K. M. *Dalton Trans.* **2009**, 1487. (c) Férey, G. *Chem. Soc. Rev.* **2008**, *37*, 191. (d) Robson, R. *Dalton Trans.* **2008**, 5113. (e) Kitagawa, S.; Matsuda, R. *Coord. Chem. Rev.* **2007**, *251*, 2490. (f) Bradshaw, D.; Claridge, J. B.; Cussen, E. J.; Prior, T. J.; Rosseinsky, M. J. *Acc. Chem. Res.* **2005**, *38*, 273. (g) Lee, S.; Mallik, A. B.;

Xu, Z.; Lobkovsky, E. B.; Tran, L. *Acc. Chem. Res.* **2005**, *38*, 251. (h) Ockwig, N. W.; Delgado-Friedrichs, O.; O'Keeffe, M.; Yaghi, O. M. *Acc. Chem. Res.* **2005**, *38*, 176. (i) Suslick, K. S.; Bhyrappa, P.; Chou, J. H.; Kosal, M. E.; Nakagaki, S.; Smithenry, D. W.; Wilson, S. R. *Acc. Chem. Res.* **2005**, *38*, 283.

(2) (a) Ma, L.; Mihalcik, D. J.; Lin, W. *J. Am. Chem. Soc.* **2009**, *131*, 4610. (b) Wang, X.-S.; Ma, S.; Forster, P. M.; Yuan, D.; Eckert, J.; López, J. J.; Murphy, B. J.; Parise, J. B.; Zhou, H.-C. *Angew. Chem., Int. Ed.* **2008**, *47*, 7263. (c) Férey, G.; Mellot-Draznieks, C.; Serre, C.; Millange, F.; Dutour, J.; Surble, S.; Margiolaki, I. *Science* **2005**, *309*, 2040. (d) Kondo, M.; Yoshitomi, T.; Seki, K.; Matsuzaka, H.; Kitagawa, S. *Angew. Chem., Int. Ed.* **1997**, *36*, 1725. (e) Huang, G.; Yang, C.; Xu, Z.; Wu, H.; Li, J.; Zeller, M.; Hunter, A. D.; Chui, S. S.-Y.; Che, C.-M. *Chem. Mater.* **2009**, *21*, 541. (f) Pan, L.; Olson, D. H.; Ciemnolonski, L. R.; Heddy, R.; Li, J. *Angew. Chem., Int. Ed.* **2006**, *45*, 616. (g) Chen, B.; Liang, C.; Yang, J.; Contreras, D. S.; Clancy, Y. L.; Lobkovsky, E. B.; Yaghi, O. M.; Dai, S. *Angew. Chem., Int. Ed.* **2006**, *45*, 1390. (h) Seo, J. S.; Whang, D.; Lee, H.; Jun, S. I.; Oh, J.; Jeon, Y. J.; Kim, K. *Nature* **2000**, *404*, 982.

(3) (a) Wu, C.-D.; Hu, A.; Zhang, L.; Lin, W. *J. Am. Chem. Soc.* **2005**, *127*, 8940. (b) Cho, S.-H.; Ma, B.; Nguyen, S. T.; Hupp, J. T.; Albrecht-Schmitt, T. E. *Chem. Commun.* **2006**, 2563. (c) Fujita, M.; Kwon, Y. J.; Washizu, S.; Ogura, K. *J. Am. Chem. Soc.* **1994**, *116*, 1151.

(4) (a) Beauvais, L. G.; Shores, M. P.; Long, J. R. *J. Am. Chem. Soc.* **2000**, *122*, 2763. (b) Zhao, B.; Chen, X.-Y.; Cheng, P.; Liao, D.-Z.; Yan, S.-P.; Jiang, Z.-H. *J. Am. Chem. Soc.* **2004**, *126*, 15394. (c) Wong, K.-L.; Law, G.-L.; Yang, Y.-Y.; Wong, W.-T. *Adv. Mater.* **2006**, *18*, 1051. (d) Chen, B.; Yang, Y.; Zapata, F.; Lin, G.; Qian, G.; Lobkovsky, E. B. *Adv. Mater.* **2007**, *19*, 1693. (e) Chen, B.; Wang, L.; Zapata, F.; Qian, G.; Lobkovsky, E. B. *J. Am. Chem. Soc.* **2008**, *130*, 6718. (f) Chen, B.; Wang, L.; Xiao, Y.; Fronczek, F. R.; Xue, M.; Cui, Y.; Qian, G. *Angew. Chem., Int. Ed.* **2009**, *48*, 500. (g) Zou, X.; Zhu, G.; Hewitt, I. J.; Sun, F.; Qiu, S. *Dalton Trans.* **2009**, 3009.

(5) (a) Southon, P. D.; Liu, L.; Fellows, E. A.; Price, D. J.; Halder, G. J.; Chapman, K. W.; Moubaraki, B.; Murray, K. S.; Létard, J.-F.; Kepert, C. J. *J. Am. Chem. Soc.* **2009**, *131*, 10998. (b) Kepert, C. J.; Prior, T. J.; Rosseinsky, M. J. *J. Am. Chem. Soc.* **2000**, *122*, 5158. (c) Kepert, C. J. *Chem. Commun.* **2006**, 695. (d) Bradshaw, D.; Prior, T. J.; Cussen, E. J.; Claridge, J. B.; Rosseinsky, M. J. *J. Am. Chem. Soc.* **2004**, *126*, 6106. (e) Zhao, X.; Xiao, B.; Fletcher, A. J.; Thomas, K. M.; Bradshaw, D.; Rosseinsky, M. J. *Science* **2004**, *306*, 1012. (f) Biradha, K.; Hongo, Y.; Fujita, M. *Angew. Chem., Int. Ed.* **2002**, *41*, 3395. (g) Kawano, M.; Fujita, M. *Coord. Chem. Rev.* **2007**, *251*, 2592. (h) Tanaka, D.; Kitagawa, S. *Chem. Mater.* **2008**, *20*, 922. (i) Atwood, J. L.; Barbour, L. J.; Jerga, A.; Schottel, B. L. *Science* **2002**, *298*, 1000. (j) Tian, J.; Thallapally, P. K.; Dalgarno, S. J.; Atwood, J. L. *J. Am. Chem. Soc.* **2009**, *131*, 13216. (k) Dobrzanska, L.; Lloyd, G. O.; Raubenheimer, H. G.; Barbour, L. J. *J. Am. Chem. Soc.* **2006**, *128*, 698. (l) Barbour, L. J. *Chem. Commun.* **2006**, 1163. (m) Zhang, Y.; Chen, B.; Fronczek, F. R.; Maverick, A. W. *Inorg. Chem.* **2008**, *47*, 4433.

(6) (a) Bradshaw, D.; Warren, J. E.; Rosseinsky, M. J. *Science* **2007**, *315*, 977. (b) Takaoka, K.; Kawano, M.; Tominaga, M.; Fujita, M. *Angew. Chem., Int. Ed.* **2005**, *44*, 2151. (c) Zhu, P.; Gu, W.; Zhang, L.-Z.; Liu, X.; Tian, J.-L.; Yan, S.-P. *Eur. J. Inorg. Chem.* **2008**, 2971. (d) Campo, J.; Falvello, L. R.; Mayoral, I.; Palacio, F.; Soler, T.; Tomás, M. *J. Am. Chem. Soc.* **2008**, *130*, 2932. (e) Ghosh, S. K.; Kaneko, W.; Kiriya, D.; Ohba, M.; Kitagawa, S. *Angew. Chem., Int. Ed.* **2008**, *47*, 8843. (f) Park, H. J.; Suh, M. P. *Chem.—Eur. J.* **2008**, *14*, 8812. (g) Zeng, M.-H.; Hu, S.; Chen, Q.; Xie, G.; Shuai, Q.; Gao, S.-L.; Tang, L.-Y. *Inorg. Chem.* **2009**, *48*, 7070. (h) Das, M. C.; Bharadwaj, P. K. *J. Am. Chem. Soc.* **2009**, *131*, 10942. (i) Matsuda, R.; Kitaura, R.; Kitagawa, S.; Kubota, Y.; Kobayashi, T. C.; Horike, S.; Takata, M. *J. Am. Chem. Soc.* **2004**, *126*, 14063. (j) Zhang, J.-P.; Lin, Y.-Y.; Zhang, W.-X.; Chen, X.-M. *J. Am. Chem. Soc.* **2005**, *127*, 14162. (k) Wu, C.-D.; Lin, W. *Angew. Chem., Int. Ed.* **2005**, *44*, 1958. (l) Nowicka, B.; Rams, M.; Stadnicka, K.; Sieklucka, B. *Inorg. Chem.* **2007**, *46*, 8123. (m) Ghosh, S. K.; Zhang, J.-P.; Kitagawa, S. *Angew. Chem., Int. Ed.* **2007**, *46*, 7965. (n) Hu, S.; He, K.-H.; Zeng, M.-H.; Zou, H.-H.; Jiang, Y.-M. *Inorg. Chem.* **2008**, *47*, 5218. (o) Libri, S.; Mahler, M.; Espallargas, G. M.; Singh, D. C. N. G.; Soleimannejad, J.; Adams, H.; Burgard, M. D.; Rath, N. P.; Brunelli, M.; Brammer, L. *Angew. Chem., Int. Ed.* **2008**, *47*, 1693. (p) Chandler, B. D.; Enright, G. D.; Udachin, K. A.; Pawsey, S.; Ripmeester, J. A.; Cramb, D. T.; Shimizu, G. K. H. *Nat. Mater.* **2008**, *7*, 229. (q) Vougo-Zanda, M.; Huang, J.; Anokhina, E.; Wang, X.; Jacobson, A. J. *Inorg. Chem.* **2008**, *47*, 11535. (r) Bernini, M. C.; Gándara, F.; Iglesias, M.; Snejko, N.; Gutiérrez-Puebla, E.; Brusau, E. V.; Narda, G. E.; Monge, M. A. *Chem.—Eur. J.* **2009**, *15*, 4896. (s) Ghosh, S. K.; Bureekaew, S.; Kitagawa, S. *Angew. Chem., Int. Ed.* **2008**, *47*, 3403. (t) Kaneko, W.; Ohba, M.; Kitagawa, S. *J. Am. Chem. Soc.* **2007**, *129*, 13706. (u) Férey, G.; Serre, C. *Chem. Soc. Rev* **2009**, *38*, 1380. (v) Vittal, J. J. *Coord. Chem. Rev.* **2007**, *251*, 1781. (w) Kitagawa, S.; Uemura, K. *Chem. Soc. Rev.* **2005**, *34*, 109.

(7) (a) Friese, V. A.; Kurth, D. G. *Coord. Chem. Rev.* **2008**, *252*, 199. (b) Ding, M.-T.; Wu, J.-Y.; Liu, Y.-H.; Lu, K.-L. *Inorg. Chem.* **2009**, *48*, 7457. (c) Wu, J.-Y.; Ding, M.-T.; Wen, Y.-S.; Liu, Y.-H.; Lu, K.-L. *Chem.—Eur. J.* **2009**, *15*, 3604. (d) Zhang, J.-J.; Zhao, Y.; Gamboa, S. A.; Lachgar, A. *Cryst. Growth Des.* **2008**, *8*, 172. (e) Zhang, J.-J.; Zhao, Y.; Gamboa, S. A.; Muñoz, M.; Lachgar, A. *Eur. J. Inorg. Chem.* **2008**, 2982. (f) Choudhury, A.; Neeraj, S.; Natarajan, S.; Rao, C. N. R. *J. Mater. Chem.* **2001**, *11*, 1537.

(8) (a) Chen, M.-S.; Chen, M.; Takamizawa, S.; Okamura, T.-a.; Fan, J.; Sun, W.-Y. *Chem. Commun.* **2011**, *47*, 3787. (b) Su, Z.; Chen, M.; Okamura, T.-a.; Chen, M.-S.; Chen, S.-S.; Sun, W.-Y. *Inorg. Chem.* **2011**, *50*, 985.

(9) Li, Y.-G.; Hao, N.; Wang, E.-B.; Lu, Y.; Hu, C.-W.; Xu, L. *Eur. J. Inorg. Chem.* **2003**, 2567.

(10) (a) Hasegawa, S.; Horike, S.; Matsuda, R.; Furukawa, S.; Mochizuki, K.; Kinoshita, Y.; Kitagawa, S. *J. Am. Chem. Soc.* **2007**, *129*, 2607. (b) Choi, E.-Y.; Park, K.; Yang, C.-M.; Kim, H.; Son, J.-H.; Lee, S. W.; Lee, Y. H.; Min, D.; Kwon, Y.-U. *Chem.—Eur. J.* **2004**, *10*, 5535.

(11) Uemura, K.; Kitagawa, S.; Kondo, M.; Fukui, K.; Kitaura, R.; Chang, H.-C.; Mizutani, T. *Chem.—Eur. J.* **2002**, *8*, 3587.

(12) (a) Xu, Z.; Lee, S.; Kiang, Y.-H.; Mallik, A. B.; Tsomaia, N.; Mueller, K. T. *Adv. Mater.* **2001**, *13*, 637. (b) Ohara, K.; Martí-Rujas, J.; Haneda, T.; Kawano, M.; Hashizume, D.; Izumi, F.; Fujita, M. *J. Am. Chem. Soc.* **2009**, *131*, 3860. (c) Jeon, Y.-M.; Heo, J.; Mirkin, C. A. *J. Am. Chem. Soc.* **2007**, *129*, 7480. (d) Uemura, K.; Kitagawa, S.; Fukui, K.; Saito, K. *J. Am. Chem. Soc.* **2004**, *126*, 3817.